ELSEVIER

Polymer 42 (2001) 9523–9529

polymer

www.elsevier.com/locate/polymer

Effects of secondary structure of fillers on the mechanical properties of silica filled rubber systems

Fumito Yatsuyanagi[a], Nozomu Suzuki[a], Masayoshi Ito[a,*], Hiroyuki Kaidou[b]

[a]*Department of Chemistry, Faculty of Science, Science University of Tokyo, 1-3 Kagurazaka, Shinjuku-ku, Tokyo, 162-8601, Japan*
[b]*Research and Development Center, The Yokohama Rubber Co. Ltd, 2-1 Oiwake, Hiratsuka, Kanagawa, 254-8601, Japan*

Received 6 March 2001; received in revised form 21 June 2001; accepted 23 June 2001

Abstract

A study was carried out on the mechanical properties of silica filled styrene–butadiene rubber systems in relation to the secondary structure formed by silica particles in the systems, which was controlled by a surface chemistry of silica particles and by a strain applied to the samples. The breakdown of the secondary structure was successfully detected by transmission electron microscopy (TEM) observations when the strain was applied to silica filled vulcanizates. The degree of breakdown was more prominent in the larger agglomerates of which the size was controlled by the number of silanol group per unit surface area of silica particles. The existence of the entrapped rubber within the agglomerate was suggested by the TEM image analysis. A part of the entrapped rubber might be released when the filler network was broken by a strain. The initial modulus of the filled rubber systems increased with the increase in the size of agglomerate. At a larger strain, the modulus decreased with the increase in the strain. The decrease was more prominent in the filled rubber, which had larger agglomerates. The reduction of modulus by the strain was closely related to the reduction of entrapped rubber phase within the agglomerates and to the breakdown of secondary structure of silica particles.

Keywords: Silica; Filled rubber; Mechanical properties

1. Introduction

Recently, silicas have been staged as a notable filler for the reinforcement of rubber composites, especially for the production of high performance passenger tires. One reason is that a silica filled passenger tire shows a low hysterisis in comparison with a carbon black filled tire [1–3].

It is well known that the carbon black filled rubber composites have multiphase systems depending on the mobility of rubber molecules, which influence the reinforcement of the composites [4–11]. Extensive works have also been carried out for the structural development in the silica filled rubber composites [12–20]. The chemical environment of silica particle is quite different from that of carbon black due to the existence of silanol groups in the particles. Thus, the primary discussion on the structural development in the silica filled rubber systems is focused on the interactions between silica particles and the interactions between silica particles and rubber molecules. Wolff and Wang studied the effects of surface energies of fillers on rubber reinforcement, and reported [14] that the surface energies of silica were characterized by a lower dispersive component and a higher specific component. The higher specific component led to strong interactions among silica particles; on the other hand, the lower dispersive component caused weak filler–rubber interactions, leading to the lower content of bound rubber in the composites and the lower moduli of the vulcanizate at a high elongation. Our transmission electron microscopy (TEM) observation of silicas revealed [20] that the averaged size of agglomerate which was formed without rubber matrix increased with the increase in the silanol number per unit surface area (N) of silica particles. Further, the silicas with low number of N ($N < 0.1$ (1/nm^2)) could not form aggregates and/or agglomerates. Qualitatively similar results were also obtained in the rubber matrix. The interesting result was that no trace of bound rubber was found in the silica filled polyisoprene composite prepared from silicas with low number of N, which might correspond to the silica with a high dispersive component. The results suggest that the formation mechanism of bound rubber in the silica filled rubber composite cannot be explained simply by the dispersive component of filler as suggested by Wolff and Wang [14]. Sawanobori et al. [20] suggest that the bound rubber in the silica filled composites exists within the agglomerate.

* Corresponding author. Tel.: +81-3-3260-4271; fax: +81-3-3235-2214.
E-mail address: maito@ch.kagu.sut.ac.jp (M. Ito).

0032-3861/01/$ - see front matter
PII: S0032-3861(01)00472-4

Table 1
Characteristics of silicas (N (1/nm^2) = SiOH (mmol/g)/Surface area (m^2/g) × Na; Na: Avogadoro number)

	AQ	ER	A-50
Diameter (nm)	18	40	50
Surface area (m^2/g)	187	78	50
SiOH (mmol/g)	1.86	0.57	0.24
N (1/nm^2)	6.0	4.4	2.9

Taking these into consideration, there is a possibility to control the size of agglomerate and the amount of bound rubber by controlling the surface chemistry of silica particles, which may influence the mechanical properties of silica filled vulcanizate.

In this study, silica filled rubber composites were prepared from several kinds of silicas having different surface chemistry and styrene–butadiene rubber. The relation between secondary structure formed by silica particles and stress–strain behavior of silica filled vulcanizates was investigated by TEM observation and mechanical testing.

2. Experimental

2.1. Samples

2.1.1. Materials

The raw rubber used was an emulsion type styrene–butadiene rubber (SBR, Nipol SBR 1502, $M_w = 430\,000$). Fillers used were two kinds of precipitate silicas (Nipsil AQ: AQ and Nipsil ER: ER), and a fumed silica (Aerosil-50: A-50). Characteristics of the silicas are listed in Table 1. The composites were prepared by a mechanical mixture.

Table 2
Compositions of filled SBR system

Sample no.	1	2	3	4
First Step				
SBR 1502	100	100	100	100
Nipsil AQ		50		
Nipsil ER			50	
Aerosil 50 (A-50)				50
Second Step				
First Master Batch	100	150	150	150
Zinc oxide	3	3	3	3
Stearic acide	2	2	2	2
Anti-oxidant 6C[a]	1	1	1	1
Third Step				
Second Master Batch	106	156	156	156
Accelerator CZ[b]	1	1	1	1
Accelerator DPG[c]	1.5	1.5	1.5	1.5
Sulfur	1.7	1.7	1.7	1.7

[a] *N*-(1,3-dimethyl butyl)-*N*′-phenyl-*p*-phenyl enediamine.
[b] *N*-Cyclohexyl-benzothiazyl-sulfenamide.
[c] Diphenyl-guanigine.

2.1.2. Mechanical mixture

As shown in Table 2, the mechanical mixture was prepared in three stages by using an internal mixer (Laboplastomill, Toyo Seiki Seisaku-shyo, Ltd). In the first stage, the masterbatch (composite) was obtained by mixing the raw rubber with silica at 100°C. In the second stage, the masterbatch was mixed with the ingredients at 80°C except sulfur and curing accelerator. In the third stage, the masterbatch obtained in the second stage was mixed with sulfur and curing accelerator at 60°C. The final stock was seated on a roll mill at 30°C followed by a vulcanization at 160°C for 30 min under a pressure.

2.1.3. Preparation of bound rubber

About 1 g of the unvulcanized mixture (the masterbatch at the first stage) that was cut into small pieces was loosely packed in a cage with 200 mesh size. The cage was immersed in a sufficiently large amount of toluene (about 300 cm^3) to remove toluene soluble rubber. The extraction was carried out at room temperature for 72 h. (There was no indication of leaching out of silica during the extraction.) The insoluble rubber component including silica (bound rubber) was suspended in acetone to exchange the toluene with more volatile chemicals and filtered. The bound rubber was dried at room temperature for three days under a reduced pressure.

2.1.4. Sample preparation for TEM observation

The samples for TEM observation were prepared from the filled vulcanizates. The ultra-thin samples (ca. 80–110 nm thick) were obtained by a microtoming of the hardened vulcanizate which was obtained by dipping the vulcanizate into sulfur at 120°C for 36 h. The hardening was carried out under the different strains applied to the vulcanizates. The uptake of sulfur was about 0.55 g per 1 g of rubber determined from element (sulfur/carbon) analyzer (EMIA-510, Horiba, Ltd). The hardened samples were microtomed in both parallel (PSD type) and vertical (VSD type) direction to the draw direction. The draw direction was perpendicular to the seating direction on the roll mill. The details are shown in Fig. 1.

2.2. Measurements

Amount of bound rubber: The amount of bound rubber (Gt, g/g) was determined as a mass of insoluble rubber per 1 g of silica. It was determined from the percentage of weight loss up to 650°C by a thermal gravimetric analyzer (TGA,TG/DTA220, Seiko Instruments).

^1H wide-line pulsed NMR: Pulsed NMR measurements were carried out with a JEOL pulsed NMR spectrometer (JNM Mu 25), operating at 25 MHz. The solid echo sequence provided a good approximation to the free induction decay (FID), from which the proton spin–spin relaxation time (T_2) was obtained. In this study, the width of 90° pulse and the pulse interval were adjusted to be 2 and 10 μs,

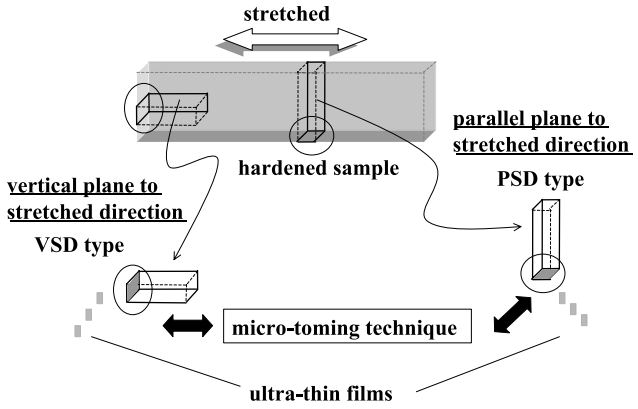

Fig. 1. Schematic representation of the direction of microtoming for the stretched sample.

respectively. Details of the NMR measurement were described in our earlier articles [6–11]. Protons in both SBR and silica contributed to the NMR signals. Thus, the signals from silica were subtracted from observed signals to make a quantitative analysis of relaxation times of rubber molecules only.

TEM observation: TEM observations were carried out by using a HITACHI H-9000 NAR Type at the accelerated voltage of 200 kV.

Stress–strain measurement: The stress–strain curves were obtained by a tensile tester (Autograph, Shimazu Seisaku-shyo, Ltd) at room temperature with the strain rate of 100%/min.

Dynamic storage modulus (E'): The dynamic storage modulus (E') was determined by a dynamic viscoelastometer (Rheolographsolid, Toyo Seiki Seisaku-sho, Ltd) at 30°C under the strain (elongation) of 0.5 ± 0.2%, and frequency of 20 Hz.

3. Results and discussion

3.1. Agglomeration of silica particles in filled SBR systems

Fig. 2 shows the typical TEM images of the samples. It is seen that the agglomerates formed by silica particles developed in the rubber matrix. The averaged size of agglomerate

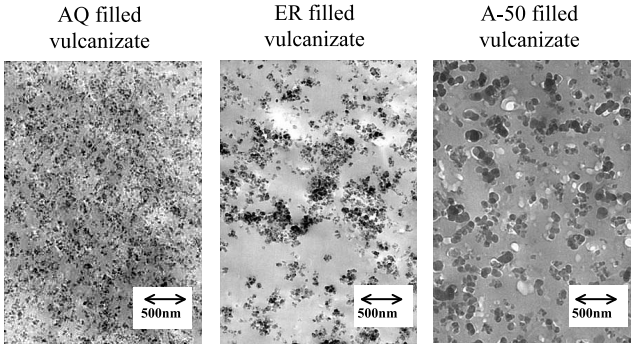

Fig. 2. TEM images of silica filled SBR vulcanizates.

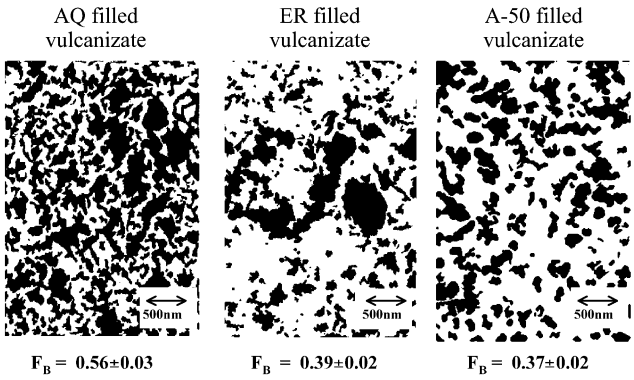

Fig. 3. TEM digital binary images of silica filled SBR vulcanizates.

and the number of silica particles which formed one agglomerate were dependent on the sort of silica. The agglomerates from AQ, which had the largest number of silanol groups per unit surface area (see Table 1), showed the largest size among the samples. On the other hand, the size for A-50, which had the smallest number of silanol group, was the smallest.

These findings were in agreement with the report by Sawanobori et al. [20] that the averaged size of agglomerate formed by silica particles in polyisoprene rubber matrix increased with the increase in the number of silanol group per unit surface area of silica surface.

3.2. TEM image analysis

A quantitative analysis of TEM images was carried out by the conversion of observed TEM images into the digital binary images [21–23]. The details are as follows: first of all, highly contrasted pictures were obtained from the observed TEM images. Then, the digital binary images were prepared from the pictures by a personal computer. In the pictures, silica particles and their agglomerates in the rubber matrix looked like a gray to dark colored phases, which were converted into black colored area. Therefore, the rest of the picture, which showed white colored portion, corresponded to the rubber matrix. The space graphic mode of the image, and the gradation sequence were 256×500 pixel and 16 bits, respectively. An indivisible flock of silica particles observed in the TEM images was defined as one agglomerate of filler particles. Fig. 3 shows the digital binary images converted from TEM images shown in Fig. 2. It is seen that the size of agglomerates became larger with the increase in the number of silanol group per unit surface area (AQ > ER > A-50) in agreement with those of the TEM images qualitatively. The area fraction of black colored portion (silica phase) of the picture (F_B) is shown at the bottom of each image. The averaged size of agglomerates ($\bar{S}_{agg}$) was also determined from the digital binary images. Both F_B and $\bar{S}_{agg}$ values were slightly affected by the magnification of the TEM observation. In this study, the binary images were obtained by using the TEM photographs with

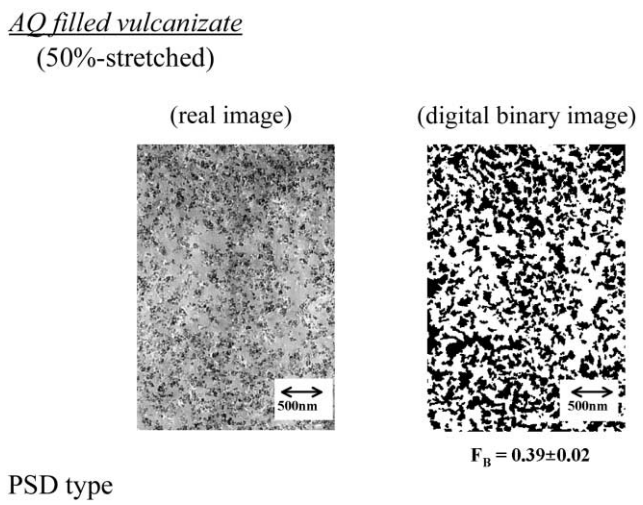

Fig. 4. TEM image and digital binary image of 50% stretched AQ filled SBR vulcanizate (PSD type).

the magnification of 20 000. In this case, the broad distribution of agglomerate size between tens of nanometers and 1 μm could be observed. When the magnification was reduced to 10 000, the agglomerate size below tens of nanometer was eliminated from TEM image due to its widespread field of view. On the other hand, under the magnification of 40 000, the heterogeneity of dispersion of silica particles was too much enhanced, and lead to the discrepancy between high and low magnifications.

As stated, the content of silica in all hardened samples was adjusted to have a similar value of ~24% by weight. Thus, all samples should have a similar value of F_B. Contrary to our expectation, the F_B increased with the increase in the size of agglomerates. In this study, the observed TEM images were converted into the digital binary images as a two-dimensional information. However,

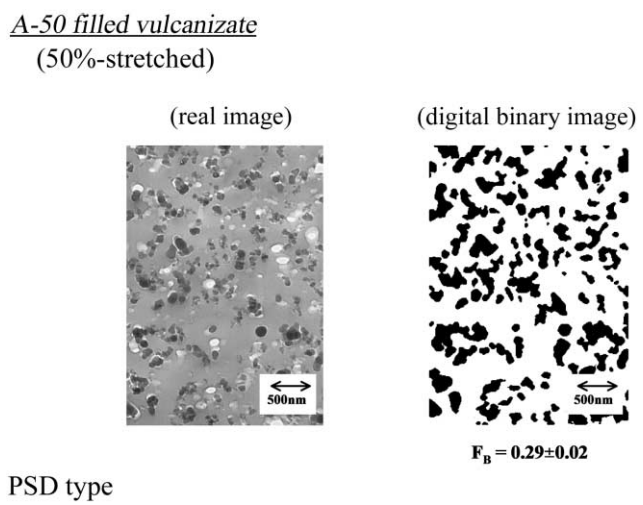

Fig. 5. TEM image and digital binary image of 50% stretched A-50 filled SBR vulcanizate (PSD type).

TEM images actually involved three-dimensional information due to the sample thickness. Thus, there is a possibility that the observed F_B value is slightly larger than the calculated one, 0.26, which was obtained under the assumption that all silica particles were sphere. As seen in Fig. 3, the difference between F_B and calculated value (0.26) is larger for the sample which has larger agglomerate (Sample no. 2, AQ filled vulcanizate) than the smaller one (Sample no. 4, A-50 filled vulcanizate). The difference of F_B between AQ and A-50 filled composites exactly exceeds the experimental error. Sawanobori et al. [20] reported that a certain amount of rubber molecules was entrapped in the agglomerates as a bound rubber in silica filled polyisoprene rubber systems. Further, the content of bound rubber increased with the increase in the size of agglomerate. In this study, the amount of bound rubber (Gt) was also determined. The Gts for AQ and A-50 filled composites were 0.65 and 0.47 (g/g), respectively. NMR results at 30°C for the bound rubber revealed that the spin–spin relaxation time (T_2) for the highly mobile rubber phase was 314 μs for AQ filled composite and 373 μs for A-50 filled composite. These T_2s were considerably short compared with that for pure SBR (about 800 μs). This means that the segmental mobility of bound rubber is highly constrained by silica particles. These results suggest that a certain amount of SBR molecules was entrapped in the agglomerates as a bound rubber similar to the case of silica filled polyisoprene composites [20]. If so, it is reasonable to consider that the F_B value is affected by the amount of bound rubber which is entrapped within the agglomerate. With the increase in the size of agglomerate, the amount of bound rubber increases, contributing to the increase in F_B.

3.3. Structural change of agglomerate by strain

Figs. 4 and 5 show TEM images and their digital binary images for the 50% stretched PSD type of ultra-thin films from AQ and A-50 filled vulcanizates. As shown in Fig. 1, two kinds of ultra-thin films were prepared (PSD and VSD types) for the TEM observation to evaluate the anisotropic effects on the structural changes of agglomerates in the silica filled vulcanizates. An example for VSD type from AQ filled vulcanizate is shown in Fig. 6. Similar to the case of PSD type, the size of agglomerate and F_B decreased by the 50% strain. Further, the decrease was almost similar to the case of PSD type (see Figs. 3 and 4). These results suggest that the stretched direction had no effect on the structural change of agglomerate in silica filled vulcanizate. The averaged sizes of agglomerate ($\bar{S}_{agg}$) and F_B values were obtained from the digital binary images for the vulcanizates with different stretch ratios and they were listed in Table 3. For both AQ and A-50 filled vulcanizates, the $\bar{S}_{agg}$ and F_B decreased with the increase in the strain with this tendency more prominent in the AQ filled vulcanizates. The changes exactly exceeded the experimental error. As described in the sample preparation, the ultra-thin samples

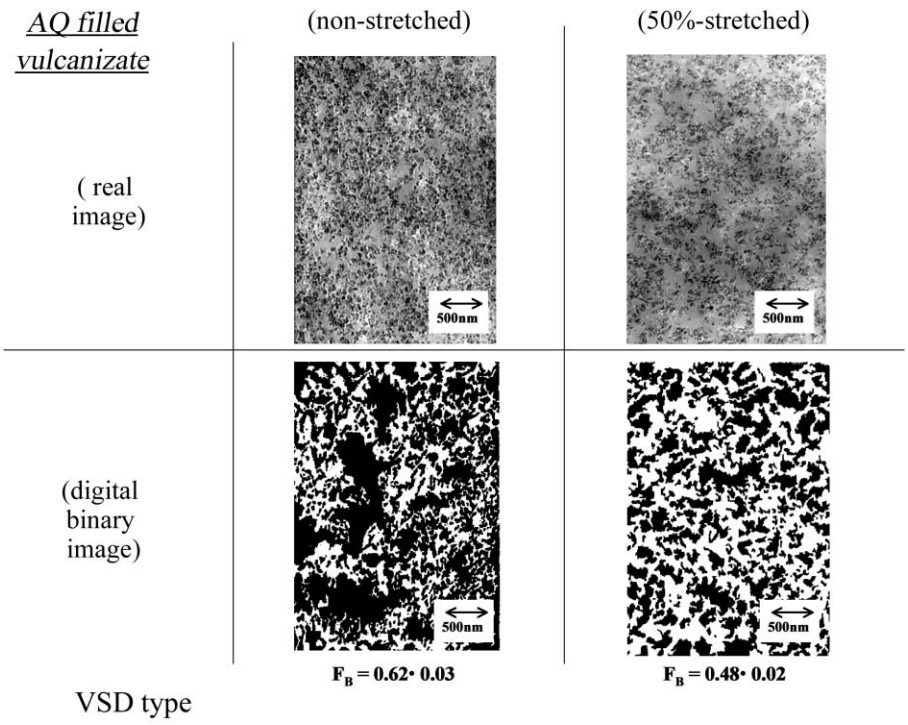

Fig. 6. TEM images and digital binary images of no stretched and 50% stretched AQ filled SBR vulcanizate (VSD type).

for TEM observations were obtained by a microtoming of the hardened vulcanizates with different stretch ratios. The structural fixation by sulfur was carried out by dipping the strained vulcanizates into sulfur at 120°C. After the vulcanization, the samples were cooled from 120°C to room temperature under the strain. After that, the strain applied to the samples was released. Then, the changes in sample size with time were checked. No change in sample size was observed just before microtoming. This means that the effect of relaxation in the rubber matrix on the structural changes of silica phase may be quite small.

3.4. Relationship between agglomerate size and mechanical properties

Fig. 7 shows the stress–strain curves of silica filled vulcanizates. The initial slope of the curves decreased with the decrease in the silanol number per unit surface area. The result indicates that the initial modulus of the samples decreases with the decrease in the agglomerate size due to the decrease in silanol number per unit surface area. Similar results were also found in the dynamic storage modulus, E', at the fine strain amplitude of $0.5 \pm 0.2\%$ (see Table 4).

Table 3
Averaged size of agglomerates ($\bar{S}_{agg}$) and area fraction of silica phase (F_B) in TEM image of silica filled vulcanizates

Stretch ratio (%)	AQ filled vulcanizate		A-50 filled vulcanziate	
	$\bar{S}_{agg}$ ($\times 10^4$ nm^2)	F_B	$\bar{S}_{agg}$ ($\times 10^4$ nm^2)	F_B
0	5.5±0.8	0.56±0.03	2.9±0.2	0.37±0.02
10	1.9±0.3	0.38±0.02	–	–
30	1.5±0.2	0.35±0.02	2.7±0.1	0.33±0.02
50	1.1±0.1	0.39±0.02	2.4±0.1	0.29±0.02

Table 4
Dynamic storage modulus (E') at fine strain amplitude in silica filled vulcanizates

	AQ filled vulcanizate	ER filled vulcanizate	A-50 filled vulcanizate	Unfilled vulcanizate
E' (MPa) at 30°C, $0.5 \pm 0.2\%$	38.9	15.8	10.5	2.7

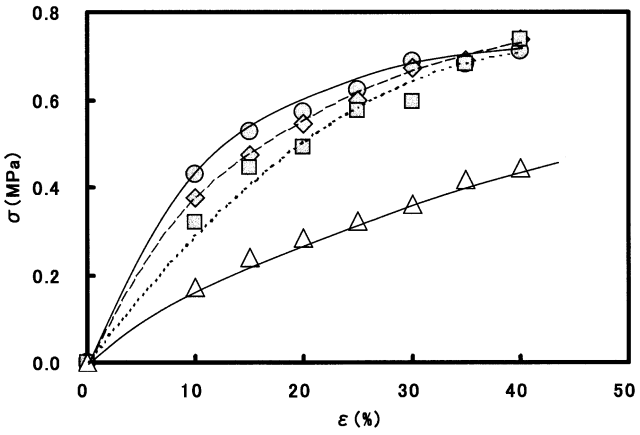

Fig. 7. Stress–strain curves at room temperature for silica filled SBR vulcanizates (circle: AQ, rhomb: ER, square: A-50, triangle: unfilled).

AQ and ER filled vulcanizates showed a pseudo-yielding point around 20% of strain. The yield phenomenon at a low strain has been thought to be the result of a breakdown of aggregates in the rubber matrix [24–28]. Around 40% of strain, all vulcanizates showed a similar stress, independent of the sort of silica.

Payne studied the effect of strain on the storage modulus for black filled vulanizate and reported [29,30] that the storage modulus of the vulcanizate decreased with the increase in strain amplitude with this tendency more prominent in the higher concentration of filler in the vulcanizate. Further, at a larger strain, the effects of filler concentration on the storage modulus became small. These results were explained by the breakdown of the aggregated secondary network of filler particles or agglomerates formed by van der Waals–London attraction forces. This consideration was supported by Kraus [31].

As stated in Section 3.3, the averaged size of agglomerate ($\bar{S}_{agg}$) for AQ filled vulcanizate was decreased by the 50% strain in accordance with the prediction by Payne [29,30]. An important result was that the area of silica phase in the vulcanizate (F_B) was also decreased by the 50% strain (see Figs. 4 and 5). As was discussed in Section 3.3, the decrease was related to the release of entrapped rubber within the agglomerates.

Based on the results and discussion, the structural change of agglomerate by the strain is shown schematically in Fig. 8. When the strain is applied to the filled vulcanizate, a breakdown of filler network occurs, which induces a decrease of agglomerate size, and simultaneously a part of the entrapped rubber within an agglomerate is released. The filler networks between silica particles themselves acquire a higher elasticity due to the hydrogen bonding between silica particles, which is presumably stronger than the van der Waals–London attractive interactions. Thus, the elasticity of the vulcanizate is decreased by the breakdown of the filler network.

The spin–spin relaxation time (T_2) of unfilled vulcanizate (Sample no. 1) was about 500 μs, which means that the segmental mobility of this sample is high. The filled vulcanizates involve agglomerates in which a certain amount of rubber is entrapped. The segmental mobility in the rubber matrix was similar to that of unfilled vulcanizate ($T_2 \sim$ 500 μs).

On the other hand, T_2 for the rubber molecules which were entrapped in the agglomerates was about 300 μs, which suggests that the segmental mobility of entrapped rubber molecules is highly constrained compared with that of rubber matrix. Thus, it is reasonable to speculate that the entrapped rubber phase is expected to show a higher elasticity compared with that of rubber matrix. By the release of entrapped rubber, the fraction of rubber phase with high elasticity in the filled vulcanizate decreases, leading to the decrease in modulus of the filled vulcanizate. Thus, the decrease in modulus by the strain arise from both the breakdown of secondary structure of filler and the release of entrapped rubber in the secondary structure.

4. Conclusions

Stress–strain measurements and TEM observations were

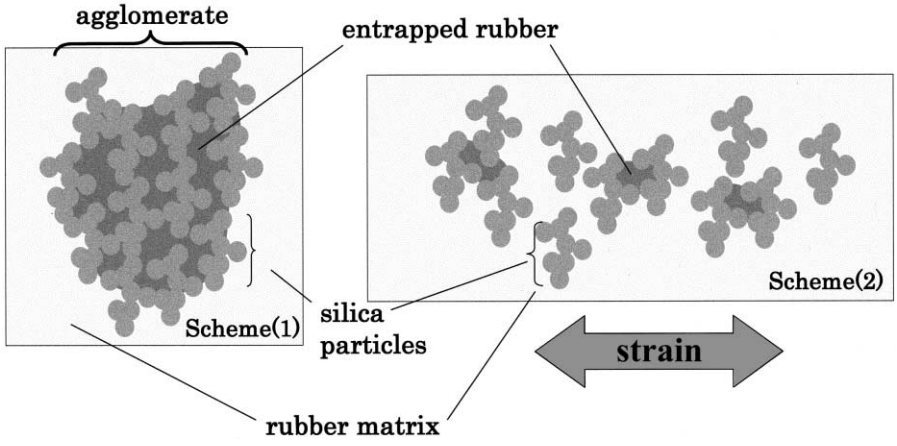

Fig. 8. Schematic representation of the breakdown of agglomerates for silica filled SBR system (Scheme 1: non stretched, Scheme 2: stretched).

carried out for silica filled vulcanizates which were prepared from different kinds of silicas. Following conclusions were derived from the experimental results:

- The breakdown of secondary structure of silica particles was successfully detected by TEM observations when the strain was applied to silica filled vulcanizates.
- The degree of breakdown was more prominent in the larger agglomerates of which the size was controlled by the silanol number per unit surface area of silica particles.
- The existence of entrapped rubber within the agglomerate was suggested by the TEM image analysis. The amount seemed to decrease with the decrease in agglomerate size. A part of the entrapped rubber might be released when the filler network was broken by the strain.
- The initial modulus of the filled vulcanizates increased with the increase in the size of agglomerate. On the other hand, at a higher strain, the modulus decreased with the increase in the strain. The decrease was more prominent in the filled vulcanizates, which had a larger size of network structure. The reduction of modulus by the strain was closely related to the reduction of entrapped rubber phase, in addition to the breakdown of secondary structure of silica particles as suggested by Payne.

Acknowledgements

The authors would like to express appreciation to Dr A. Ahagon for his valuable discussion through this work and to Dr N. Miyashita for his help for the TEM image analysis in The Yokohama Rubber Co., Ltd. Special thanks are extended to The Yokohama Rubber Co., Ltd for granting permission to publish this paper.

References

[1] Hensel M, Menting K-H, Umland H, Stone C. Tire Technol Int 1997:124.
[2] The Smither's Report 1998;10:3.
[3] Mouri H, Akutagawa K. Rubber Chem Technol 1999;72:960.
[4] Kaufman S, Slicter WP, Daivis DD. J Polym Sci 1976;A-2:9:829.
[5] O'Brien J, Cashel E, Wardell GE, McBrierty VJ. Macromolecules 1976;9:653.
[6] Serizawa H, Ito M, Kanamoto T, Tanaka K, Nomura A. Polym J 1982;14:149.
[7] Yatsuyanagi F, Kaidou H, Ito M. J Soc Rubber Ind Jpn 1994;67:707.
[8] Kida N, Ito M, Yatsuyanagi F, Kaidou H. J Appl Polym Sci 1996;61:1345.
[9] Yatsuyanagi F, Kaidou H, Kida N, Ito M. J Soc Rubber Ind Jpn 1997;70:274.
[10] Yatsuyanagi F, Kaidou H, Ito M. Rubber Chem Technol 1999;72:657.
[11] Kiuchi Y, Ito M. J Soc Rubber Ind Jpn 1999;72:599.
[12] Ito M, Nakamura T, Tanaka K. J Appl Polym Sci 1985;30:3493.
[13] Kralevich ML, Koenig JL. Rubber Chem Technol 1998;71:300.
[14] Wolff S, Wang M-J. Rubber Chem Technol 1992;65:329.
[15] Wolff S. Rubber Chem Technol 1996;69:325.
[16] Wolff S, Donnet J-B. Rubber Chem Technol 1990;63:32.
[17] Wolff S, Wang M-J, Tan E-H. KGK Kaut Gum Kunst 1994;47:102.
[18] Ono S, Kiuchi Y, Sawanobori J, Ito M. Polym Int 1999;48:1035.
[19] Ono S, Ito M, Tokumitsu H, Seki K. J Appl Polym Sci 1999;74:2529.
[20] Sawanobori J, Ono S, Ito M. Jpn J Polym Sci Technol 2000;57:356.
[21] Tanaka H, Hyasshi T, Nishi T. J Appl Phys 1986;59:653.
[22] Tanaka H, Hyasshi T, Nishi T. J Appl Phys 1989;65:4480.
[23] Hayashi T, Watanabe A, Tanaka H, Nishi T. Jpn J Polym Sci Technol 1992;49:373.
[24] Bachmann JH, Shellers JW, Wagner MP, Wolf RF. Rubber Chem Technol 1959;32:1286.
[25] Wagner MP. Rubber Chem Technol 1976;49:703.
[26] Waddell WH, Beauregard PA, Evans LR. Tire Technol Int 1995:24.
[27] Bueche AM. J Appl Polym Sci 1961;5:271.
[28] Bueche AM. In: Kraus G, editor. Network theory of reinforcement in reinforcement of elastomers. New York: Interscience, 1965.
[29] Payne AR. In: Kraus G, editor. Dynamic properties of filler-loaded rubbers in reinforcement of elastomers. New York: Interscience, 1965.
[30] Payne AR, Whittaker RE. Rubber Chem Technol 1971;44:440.
[31] Kraus G. J Appl Polym Sci: Appl Polym Symp 1984;39:75.